

2020 July Sea Ice Outlook Supplementary Report ECCC-CanSIPsv2

Bill Merryfield¹, Arlan Dirkson², Cathy Reader¹, Hai Lin³, Marko Markovich³, Michael Sigmond¹,
Woosung Lee¹

¹Environment and Climate Change Canada, Canadian Centre for Climate Modeling and Analysis

²Universite du Quebec a Montreal

³Environment and Climate Change Canada, Canadian Centre for Meteorological and Environmental Prediction

Outlook Summary and Methods:

Our outlook includes an estimate of pan-Arctic sea ice extent (SIE), as well as spatial forecast fields of sea ice probability (SIP), sea ice concentration (SIC), and ice-free dates (IFDs). The outlook was produced using the Canadian Seasonal to Interannual Prediction System (CanSIPv2; Lin et al., 2020: <https://doi.org/10.1175/WAF-D-19-0259.1>), which combines ensemble forecasts from two models, CanCM4i and GEM-NEMO, with a total of 20 ensemble members (10 from each model). Our pan-Arctic SIE estimate was formulated by calculating (for each ensemble member) the SIE anomaly relative to a piecewise linear trend fitted to the respective model's ensemble-mean SIE time series over 1980-2019. These anomalies were then added to the fitted piecewise linear trend for the NSIDC sea ice index SIE time series, and then averaged over all 20 ensemble members to yield a total SIE of 4.36 million square kilometers. The piecewise linear fit, including the breakpoint year, was found using non-linear least squares. Sea ice probability maps were produced by first calibrating the ensemble SIC forecasts for each respective model using trend-adjusted quantile mapping (TAQM; Dirkson et al., 2019: <https://doi.org/10.1175/JCLI-D-18-0224.1>), computing the probability for SIC>15%, and then averaging those probabilities across both models. Our outlook for the 80% SIC contour was prepared by first bias correcting the full ensemble SIC fields for each model separately using a 2011-2019 baseline, and then averaging the ensemble mean SIC across both models. The resultant SIC field was then converted to 0's and 1's corresponding to which grid cells have SIC<80% and which have SIC>=80%, respectively. Similarly, our IFD forecast has been bias-corrected based on the 2011-2019 mean IFD, where we have defined the IFD as the first date that SIC falls below 50% and remains below that value for 10 consecutive days (Sigmond et al., 2016: <https://doi.org/10.1002/2016GL071396>).

Pan-Arctic SIE: 4.36 million sq. km (95% CI=3.81,4.91)

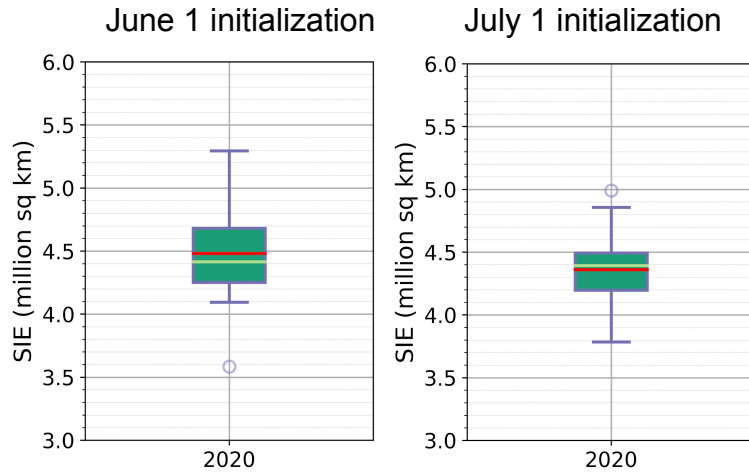


Figure 1 Box-and-whisker diagram of CanSIPsv2 forecast September mean SIE using initial conditions from June 1 (left) and July 1 (right); box=Q1 to Q2; whiskers= Q1 - 1.5*IQR to Q3 + 1.5*IQR; dots=outliers; red line = ensemble mean; lime green line = ensemble median. Note: the 95% confidence interval in red text was obtained by approximating the forecast ensemble as a Gaussian distribution. The ensemble mean SIE from July 1 is slightly lower than that estimated from June 1, and there is expectedly higher confidence in the forecast

Historical context and past skill:

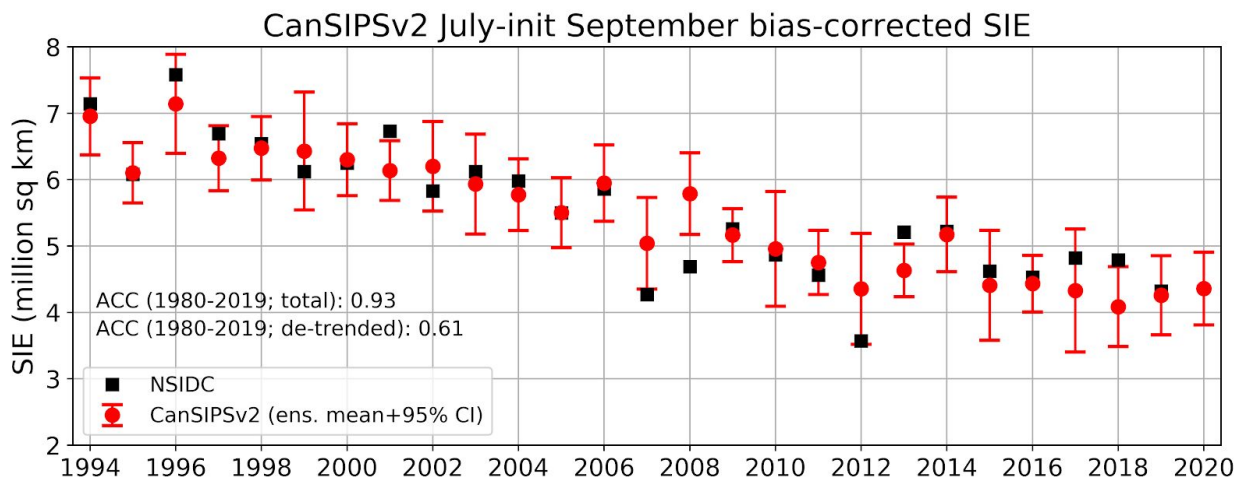


Figure 2 Bias-corrected CanSIPsv2 hindcasts of September mean SIE from 1994-2020. Skill estimates provided (ACC = anomaly correlation coefficient) were computed using the full hindcast record from 1980-2019. The linearly de-trended correlation for hindcasts initialized on July 1 is 0.1 units larger (more skillful) than hindcasts from June 1.

Sea Ice Concentration:

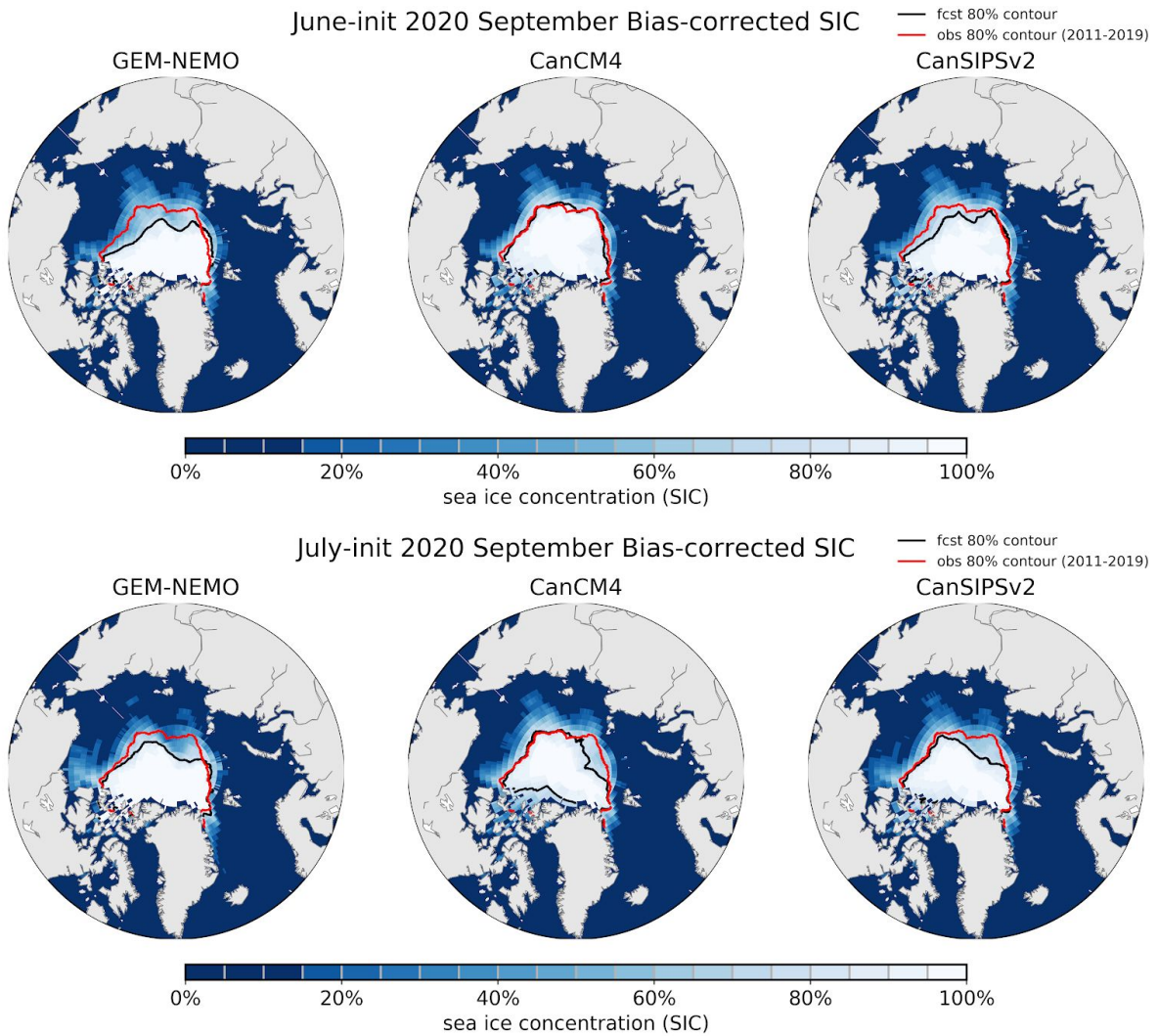


Figure 3. Bias-corrected ensemble-mean sea ice concentration forecast for September, 2020, for GEM-NEMO, CanCM4i, and (their combination) CanSIPsv2. The top row shows the June 1 initialized forecast, whereas the bottom row shows the forecast initialized on July 1. The forecast 80% contour in the Fram Strait is very consistent between the two forecasts.

Sea Ice Probability

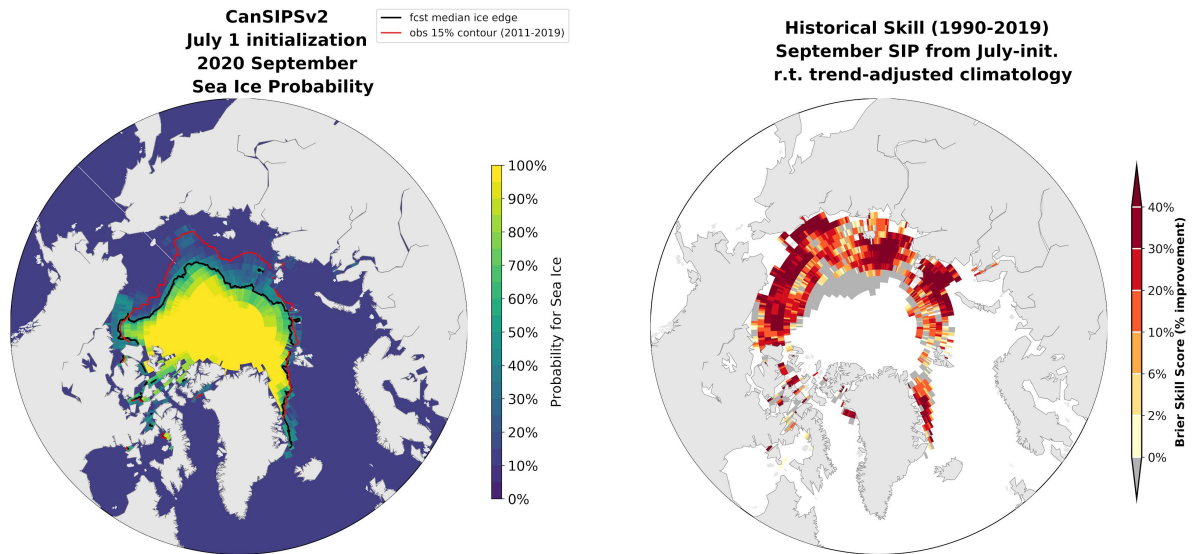


Figure 4. Left: Probability for ice concentration greater than 15%; Right: Historical skill based on the Brier skill score over the period 1990-2019, where skill is quantified relative to a trend-adjusted climatology.

Ice-Free Date Forecast

Ensemble-mean (deterministic) forecast:

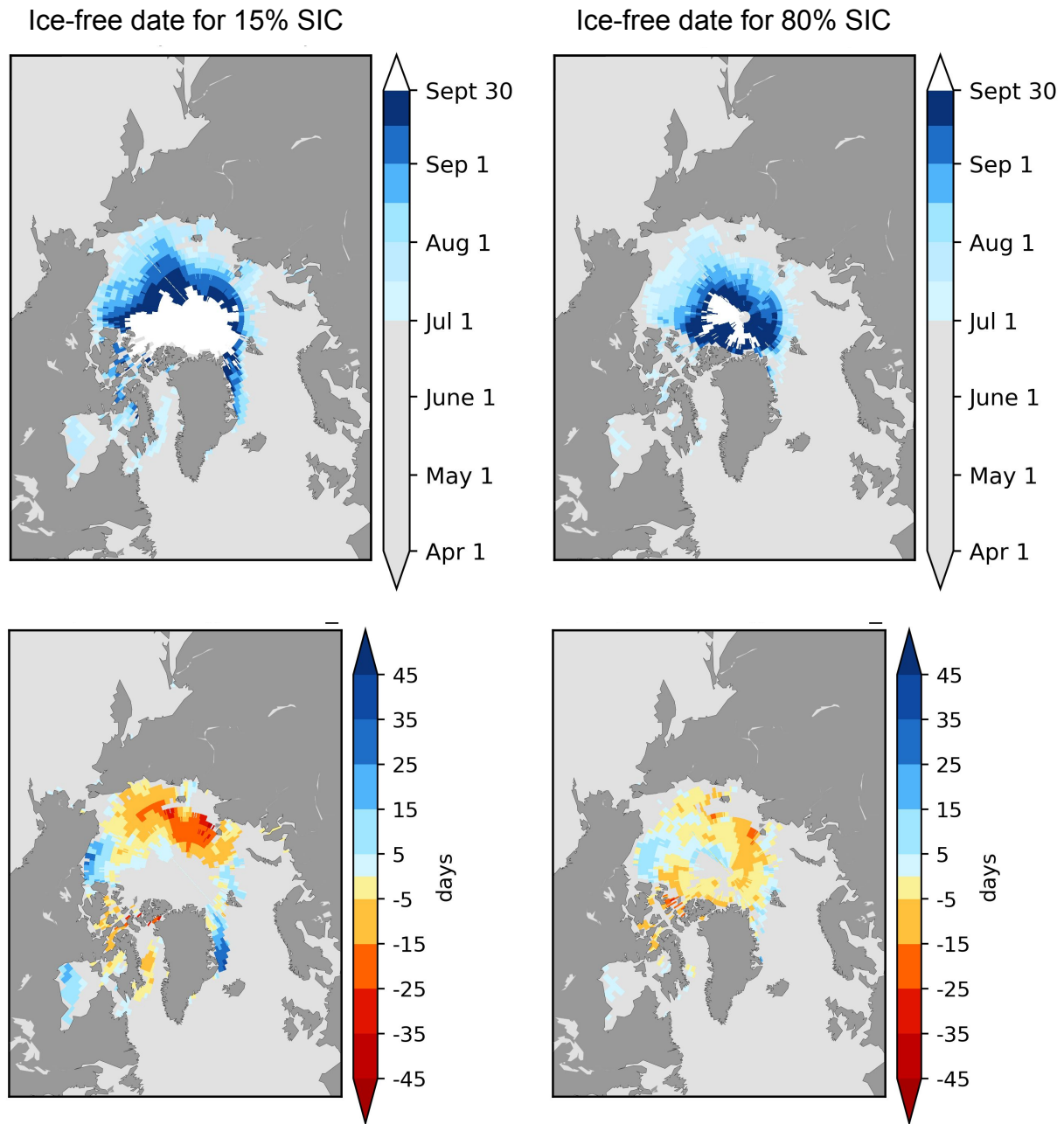


Figure 5. Bias-corrected ice-free date forecasts (top) and anomalies relative to the 2011-2019 average observed date (bottom). Like the forecasts initialized on June 1, late ice retreat is still forecast to happen in the southern Hudson Bay, Beaufort Sea, southern Fram Strait, and southern Barents Sea; elsewhere early retreat dates are forecast, with a stronger signal for early retreat now in the Laptev Sea to the north of where ice has already retreated.

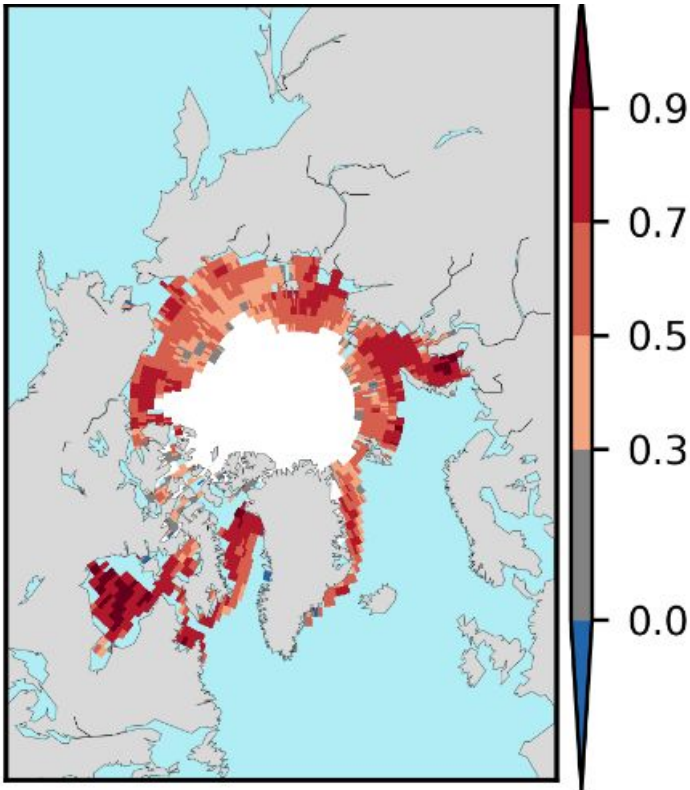


Figure 6. Historical ice-free date forecast skill over the period 1980-2019 from July 1, based on the anomaly correlation coefficient computed after linearly de-trending the hindcast and observed IFDs. The skill map is for ice break-up according to when ice concentration falls below 50%. The generally high skill indicates that CanSIPsv2 IFD forecasts can be well trusted in most regions.

Ice-Free Date Forecast

New experimental probabilistic IFD forecast

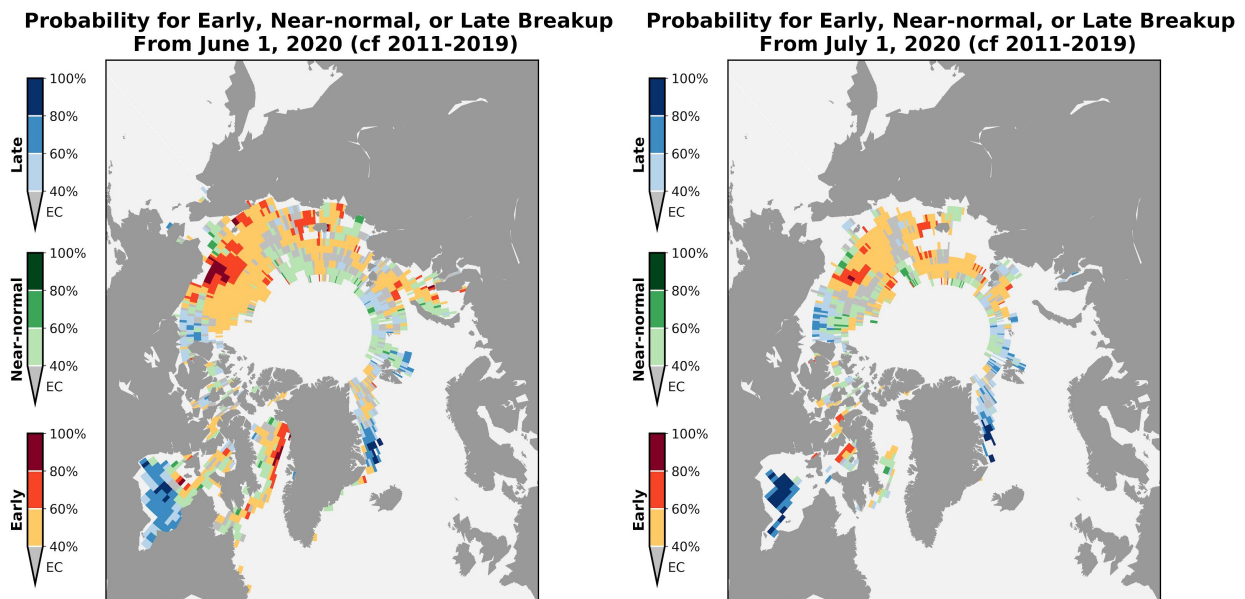


Figure 7. Probabilistic forecast for early, near-normal, or late sea-ice retreat (the most likely category is plotted at each grid point) from forecasts made on June 1 (left) and July 1 (right), according to when ice concentration falls below 50%. The forecast probabilities for each category are computed relative to the observed dates over the last 9 years (~earliest 3, middle 3, latest 3); EC=equal chances. The ensemble IFD at each grid point was calibrated using “non-homogenous censored Gaussian regression” (NCGR; Dirkson et al., under review @ WaF), a newly-developed calibration method designed specifically for IFD and freeze-up date forecasts.